Correction

SUSTAINABILITY SCIENCE

Correction for "Quantifying the hurricane risk to offshore wind turbines," by Stephen Rose, Paulina Jaramillo, Mitchell J. Small, Iris Grossmann, and Jay Apt, which appeared in issue 9, February 28, 2012, of *Proc Natl Acad Sci USA* (109:3247–3252; first published February 13, 2012; 10.1073/pnas.1111769109).

The authors note that on page 3251, right column, Equations **6** and **8** appeared incorrectly. The corrected equations appear below. These errors do not affect the conclusions of the article.

$$T_{ij}(y,n) = \lambda\ \text{beta} - \text{binomial}(n-i+1, (n-i+1)-(n-j+1);\ \alpha_B, \beta_B) \quad j > i \qquad \textbf{[6]}$$

$$t_i(y,n) = \lambda \sum_{m=0}^{n-y-1} \text{beta} - \text{binomial}(n-i+1, (n-i+1)-m; \alpha_B, \beta_B) \qquad \textbf{[8]}$$

www.pnas.org/cgi/doi/10.1073/pnas.1211974109

Quantifying the hurricane risk to offshore wind turbines

Stephen Rose[a], Paulina Jaramillo[a,1], Mitchell J. Small[a,b], Iris Grossmann[a], and Jay Apt[a,c]

[a]Department of Engineering and Public Policy; [b]Department of Civil and Environmental Engineering; and [c]Tepper School of Business, Carnegie Mellon University, 5000 Forbes Avenue, Pittsburgh, PA 15213

Edited by William C. Clark, Harvard University, Cambridge, MA, and approved January 10, 2012 (received for review July 19, 2011)

The U.S. Department of Energy has estimated that if the United States is to generate 20% of its electricity from wind, over 50 GW will be required from shallow offshore turbines. Hurricanes are a potential risk to these turbines. Turbine tower buckling has been observed in typhoons, but no offshore wind turbines have yet been built in the United States. We present a probabilistic model to estimate the number of turbines that would be destroyed by hurricanes in an offshore wind farm. We apply this model to estimate the risk to offshore wind farms in four representative locations in the Atlantic and Gulf Coastal waters of the United States. In the most vulnerable areas now being actively considered by developers, nearly half the turbines in a farm are likely to be destroyed in a 20-y period. Reasonable mitigation measures—increasing the design reference wind load, ensuring that the nacelle can be turned into rapidly changing winds, and building most wind plants in the areas with lower risk—can greatly enhance the probability that offshore wind can help to meet the United States' electricity needs.

probabilistic analysis | wind energy | phase-type distribution | tropical cyclone

As a result of state renewable portfolio standards and federal tax incentives, there is growing interest and investment in renewable sources of electricity in the United States. Wind is the renewable resource with the largest installed-capacity growth in the last 5 y, with U.S. wind power capacity increasing from 8.7 GW in 2005 to 39.1 GW 2010 (1). All of this development has occurred onshore. U.S. offshore wind resources may also prove to be a significant contribution to increasing the supply of renewable, low-carbon electricity. The National Renewable Energy Laboratory (NREL) estimates that offshore wind resources can be as high as four times the U.S. electricity generating capacity in 2010 (2). Although this estimate does not take into account siting, stakeholder, and regulatory constraints, it indicates that U.S. offshore wind resources are significant. Though no offshore wind projects have been developed in the United States, there are 20 offshore wind projects in the planning process (with an estimated capacity of 2 GW) (2). The U.S. Department of Energy's 2008 report, *20% Wind by 2030* (3) envisions 54 GW of shallow offshore wind capacity to optimize delivered generation and transmission costs.

U.S. offshore resources are geographically distributed through the Atlantic, Pacific, and Great Lake coasts. The most accessible shallow resources are located in the Atlantic and Gulf Coasts. Resources at depths shallower than 60 m in the Atlantic coast, from Georgia to Maine, are estimated to be 920 GW; the estimate for these resources in the Gulf coast is 460 GW (2).

Offshore wind turbines in these areas will be at risk from Atlantic hurricanes. Between 1949 and 2006, 93 hurricanes struck the U.S. mainland according to the HURDAT (Hurricane Database) database of the National Hurricane Center (4). In this 58-y period, only 15 y did not incur insured hurricane-related losses (5). The Texas region was affected by 35 hurricane events, while the southeast region [including the coasts of Florida, where no offshore resources have been estimated (2)] had 32 events.

Hurricane risks are quite variable, both geographically and temporally. Pielke, et al. (6) note pronounced differences in the total hurricane damages (normalized to 2005) occurring each decade. Previous research has shown strong associations between North Atlantic hurricane activity and atmosphere-ocean variability on different time scales, including the multidecadal (7, 8). Atlantic hurricane data show that hurricane seasons with very high activity levels occur with some regularity; for instance, since 1950, there have been 25 y with three or more intense hurricanes (Saffir-Simpson Category 3 or higher). There were two 2-y periods with 13 intense hurricanes: 1950–1951 and 2004–2005. 2004 and 2005 hurricanes were particularly damaging to the Florida and Gulf Coast regions (six hurricanes made landfall in those areas in 2004 and seven the following year).

These hurricanes resulted in critical damages to energy infrastructure. Hurricane Katrina (2005), for example, was reported to have damaged 21 oil and gas producing platforms and completely destroyed 44 (9). Numerous drilling rigs and hydrocarbon pipelines were also damaged. Similarly, hurricanes have damaged powers systems. Liu, et al. (10) reported that in 2003 Dominion Power had over 58,000 instances of the activation of safety devices in the electrical system to isolate damages as a result of Hurricane Isabel. Although no offshore wind turbines have been built in the United States, there is no reason to believe that this infrastructure would be exempt from hurricane damages.

In order to successfully develop sustainable offshore resources, the risk from hurricanes to offshore wind turbines should be analyzed and understood. Here we present a probabilistic model to estimate the number of turbines that would be destroyed by hurricanes in an offshore wind farm. We apply this model to estimate the risk to offshore wind farms in four representative locations in the Atlantic and Gulf Coastal waters of the United States: Galveston County, TX; Dare County, NC; Atlantic County, NJ; and Dukes County, MA. Leases have been signed for wind farms off the coasts of Galveston (11) and Dukes County (12); projects off the coasts of New Jersey and North Carolina have been proposed (12).

Results

Wind Farm Risk from a Single Hurricane. Wind turbines are vulnerable to hurricanes because the maximum wind speeds in those storms can exceed the design limits of wind turbines. Failure modes can include loss of blades and buckling of the supporting tower. In 2003, a wind farm of seven turbines in Okinawa, Japan was destroyed by typhoon Maemi (13) and several turbines in China were damaged by typhoon Dujuan (14). Here we consider only tower buckling, because blades are relatively easy to replace

Author contributions: S.R., P.J., M.J.S., and J.A. designed research; S.R. performed research; I.G. contributed the meteorological component; S.R., P.J., M.J.S., and J.A. analyzed data; and S.R., P.J., I.G., and J.A. wrote the paper.

The authors declare no conflict of interest.

This article is a PNAS Direct Submission.

[1]To whom correspondence should be addressed. E-mail: paulina@cmu.edu.

This article contains supporting information online at www.pnas.org/lookup/suppl/doi:10.1073/pnas.1111769109/-/DCSupplemental.

SUSTAINABILITY SCIENCE

(although their loss can cause other structural damage). To illustrate the risk to a wind farm from hurricane force wind speeds, we calculate the expected number of turbine towers that buckle in a 50-turbine wind farm as a function of maximum sustained (10-min mean) wind speed, assuming that turbines cannot yaw during the hurricane to track the wind direction (we later consider the case in which the nacelle can be yawed rapidly enough to track the wind direction of the hurricane). Fig. 1 plots the median, fifth percentile, and 95th percentile of the number of turbine towers that buckle as a function of wind speed. The vertical dotted line shows the design reference wind speed for wind turbines in IEC (International Electrotechnical Commission) Class 1 wind regimes, which includes the NREL 5-MW turbine we simulate, and nearly all offshore wind turbines currently in production. The IEC 61400-3 design standard for Class 1 wind regimes requires that a turbine survive a maximum 10-min average wind speed with a 50-y return period of 50 m/s (97 knots) at hub height (15); we scale this wind speed from 90-m height to 10-m height assuming power-law wind shear with an exponent of 0.077 (16) because hurricane wind speeds are given for 10-m height.

A Category 2 hurricane (wind speeds of 45 m/s or higher) will buckle up to 6% of the turbine towers in a wind farm. Hurricane Ike in 2008, for example, had a maximum sustained wind speed of 95 knots (49 m/s) at 10-m height (Category 2) when it passed over the meteorological tower erected by the developers of the Galveston Offshore Wind project. If a 50-turbine wind farm had been located off the coast of Galveston when Hurricane Ike struck, our model predicts that Hurricane Ike would have had a 50% probability of buckling two or more towers and a 10% probability of buckling four or more turbine towers.

Higher-category hurricanes will destroy a significant number of turbines; a Category 3 (wind speeds of 50 m/s or higher) will buckle up to 46% of the towers. The damage caused by Category 3, 4, and 5 hurricanes is important for offshore wind development in the United States because every state on the Gulf of Mexico coast and 9 of the 14 states on the Atlantic Coast have been struck by a Category 3 or higher hurricane between 1856 and 2008 (17).

Risk from Multiple Hurricanes. We calculate the cumulative distribution function (CDF) for the number of turbine towers that buckle in 20 y for wind farms at four different locations, assuming that buckled towers are not replaced after each storm. The distributions are modeled by a modified phase-type distribution described in *Materials and Methods*. Fig. 2 shows the CDF for each location for two cases: turbines that can yaw to track wind direction (dashed line) and turbines that cannot yaw (solid line). The nonyawing case is a worst case scenario, but it is realistic for two reasons. First, wind turbines typically do not have backup power for yaw motors and hurricanes often cause widespread power outages. Wind turbine design standards such as the IEC 61400-3 (Design Load Case 6.2) require turbine designers to assume a yaw misalignment up to ±180° if no yaw backup power is available, though designers can assume the turbine points directly into the wind if 6 h of backup power is available for the yaw and control systems (15). Second, wind direction in a hurricane may change faster than a wind turbine can yaw. The NREL 5-MW turbine we model is designed to yaw at 0.3°/sec, but Schroeder, et al. show that the wind direction of Hurricane Bob in 1991 changed 30° in approximately 60 s (0.5°/sec), as measured 55 km away from the center of the storm (18). The yawing case in Fig. 2 illustrates how much the risk to a wind farm is reduced if the turbines can track the wind direction quickly and reliably as a hurricane passes.

Galveston County is the riskiest location to build a wind farm of the four locations examined, followed by Dare County, NC. In contrast, Atlantic County, NJ and Dukes County, MA are significantly less risky. In Galveston County, there is a 60% probability that at least one tower will buckle in 20 y and a 30% probability that more than half will buckle if the turbines cannot yaw; if they are able to yaw, there is still a 25% probability that at least one tower will buckle and a 10% probability that more than half will. In Dare County, NC, there is a 60% probability that at least one tower will buckle in 20 y and a 9% probability that more than half will buckle if the turbines cannot yaw; if they are able to yaw, there is a 15% probability that at least one tower will buckle and much less than 1% probability that more than half will.

In Atlantic County, NJ there is a 15% probability that at least one tower will buckle in 20 y and less than 1% probability that more than half will buckle. In Dukes County, MA, there is a 10% probability that at least one tower will buckle in 20 y and less than 1% probability that more than half will buckle. If the turbines in Atlantic and Dukes counties are able to quickly yaw even when grid power is out, there is approximately a 99% probability that none will buckle in 20 y.

The results in Fig. 2 assume the TI of hurricanes is lognormally distributed with a mean of 9% and standard deviation of 1.5%, where we define the turbulence intensity (TI) as the 10-min standard deviation of wind speed divided by the 10-min mean wind speed. The TI distribution is fitted to data from tropical cyclones over water, as discussed in the *SI Text*. The probability distributions in Fig. 2 are sensitive to the chosen value of TI: higher turbulence intensities for a given mean wind speed means higher

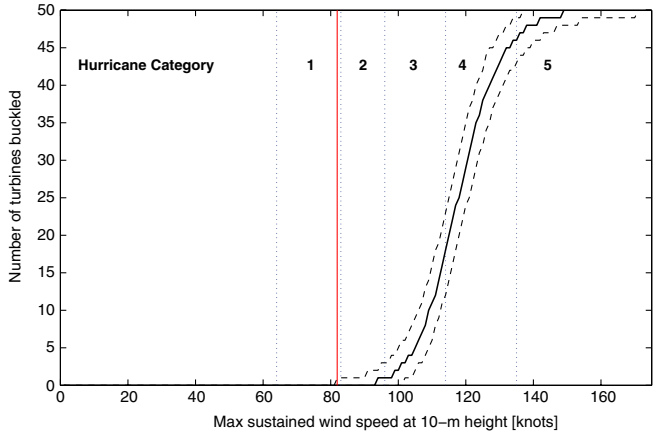

Fig. 1. Cumulative distribution function of the expected number of turbine towers buckled by a single storm as a function of wind speed. This models a hurricane with a TI of 9% in a 50-turbine wind farm of NREL 5-MW turbines (35) that cannot yaw to track the wind. The dashed lines plot the 5th and 95th percentile values and the solid vertical line shows V_{ref}, the design wind speed with a 50-yreturn period (15) scaled to 10-m height.

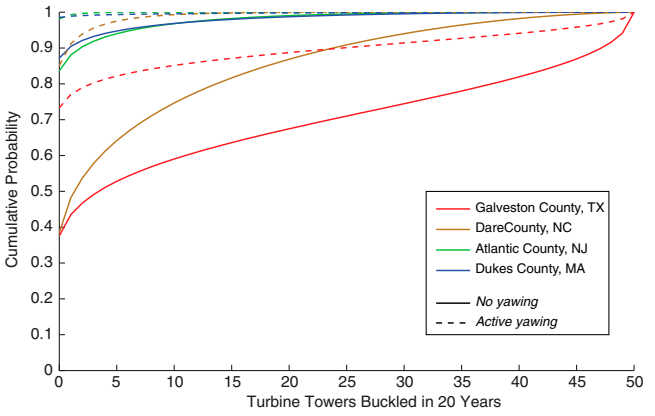

Fig. 2. Cumulative distribution of the number of turbine towers in a 50-turbine wind farm buckled in 20 y if buckled towers are not replaced. Dashed lines plot the distribution for the case that turbines can yaw to track the wind direction, and solid lines plot the distribution for the case that turbines cannot yaw.

peak wind speeds, which increase the probability of a turbine tower buckling.

If turbines are replaced after each hurricane, the cumulative probabilities for fewer than 35 turbine towers buckling in 20 y is within four percentage points of the distributions without replacement shown in Fig. 2. However, there is a possibility that more than 50 turbine towers will buckle in 20 y. For example, there is a 10% probability in Galveston County and 1% probability in Dare County that more than 50 turbine towers will buckle if the turbines cannot yaw. The distributions with replacement are modeled as a compound Poisson distribution; the derivation of the distribution and a CDF plot of the results are given in *SI Text*.

Distribution of Damage by Hurricane Intensity. The number of turbine towers that buckle in a wind farm during the farm's 20-y life is a function of the frequency of hurricane occurrence and the intensity of the hurricanes that occur. Higher-intensity storms buckle more turbine towers, but occur less frequently. To assess which categories of hurricanes cause the most expected damage, we use Monte Carlo simulation to calculate the expected value of the number of turbines that buckle in 20 y and the expected damage from each category of hurricane. The results are plotted in Fig. 3. These results reflect damages averaged through 10,000 simulated 20-y periods. The results in any given 20-y period will be different, typically dominated by one or two hurricanes.

Fig. 3 indicates that Category 3, 4, and 5 hurricanes are projected to cause most of the expected damage at each location: 98% in Galveston County, 95% in Dare County, 92% in Atlantic County, and 92% in Dukes County. However, no Category 4 and 5 hurricanes have made landfall in Dare, Atlantic, or Dukes counties since record keeping began in 1850. Analyses of U.S. hurricanes prior to 1850 report four landfalls in North Carolina that may have been Category 4 (in 1815, 1827, 1842, and 1846) (19, 20) and one in 1821 that was likely either Category 4 or 5 (20). This historic record indicates that hurricanes of intensity 4 or higher should be possible in Dare County. Category 4 hurricanes also appear possible in Atlantic County with sufficiently warm sea-surface temperatures such as during late August. Hurricane model projections (19) indicate that the Great Colonial Hurricane of August 1635 most likely retained Category 4 intensity until reaching southern New Jersey. However, storms of Category 4 intensity in coastal Massachusetts may be physically impossible in present climate conditions. Generalized Extreme Value distributions (GEV) fit to the maximum sustained wind speeds of hurricanes in the regions around Dare, Atlantic, and Dukes counties predict probabilities of 4%, 2%, and 2%, respectively, that a hurricane making landfall in those counties will be Category 4 or 5.

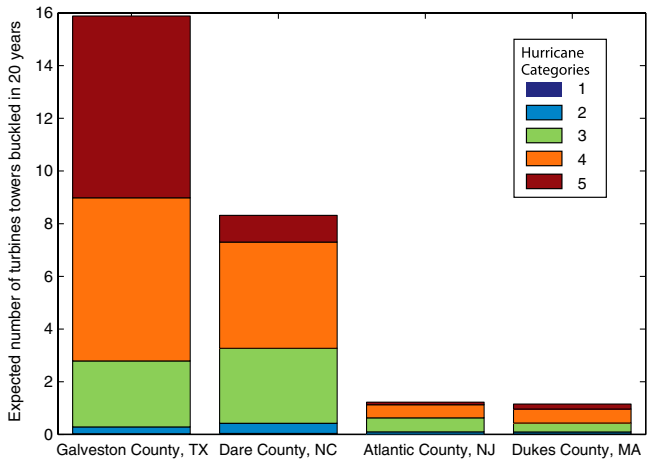

Fig. 3. The expected number of turbine towers that buckle in a 50-turbine wind farm over 20 y for each location, subdivided by hurricane category.

We test the sensitivity of our results in Fig. 2 and Fig. 3 to the occurrence of Category 4 and 5 hurricanes by repeating the Monte Carlo simulation of 10,000 20-y periods but excluding periods that contain a Category 4 or 5 hurricane. This analysis excludes 16% of total simulations for Dare County, 2% for Atlantic County, and 2% for Dukes County. The results for Dare County are the most sensitive to the occurrence of high-category hurricanes: the expected number of turbine towers that buckle in 20 y decreases from 8.3 to 3.2, the probability of no turbine towers buckling increases from 33% to 39%, and the probability that less than half the turbine towers buckle increases from 89% to more than 99% when Category 4 and 5 hurricanes are excluded. The results for Atlantic and Dukes counties show a similar trend: the expected number of turbine towers that buckle falls from 1.3 to 0.6 in Atlantic County and from 1.2 to 0.5 in Dukes County. In both Atlantic and Dukes counties, the probabilities of none of the turbine towers and less than half the turbine towers buckling increase approximately two percentage points. Plots of the CDF of number of turbine towers bucked with higher-category hurricanes excluded are given in *SI Text*.

Discussion

The 2008 DOE (Department of Energy) report (3) estimates that 54 GW of shallow offshore wind capacity will be required to bring the United States to 20% wind, and locates most of that capacity off the Gulf and East coasts. We find that hurricanes pose a significant risk to wind turbines off the U.S. Gulf and East coasts, even if they are designed to the most stringent current standard (IEC Class 1 winds). Now is an appropriate moment to consider mitigation strategies that can be incorporated to reduce risk to the grid and to operators, before large-scale offshore wind development is undertaken in the United States.

Engineered solutions can mitigate the risk of wind turbine damage as a result of hurricanes in the eastern United States. Typically, wind turbines are designed based on engineering design codes for northern Europe and the North Sea, where nearly all the offshore and coastal wind turbines have been built. These codes specify maximum sustained wind speeds with a 50-y return period of 42.5–51.4 m/s (83–100 knots), lower than high intensity hurricanes (21). Several authors have studied extreme winds in areas prone to tropical cyclones. Garciano, et al. (22), propose increasing the 50-y design reference wind speed for the Philippines from 50 m/s to 58 m/s at hub height, Clausen, et al. (23), propose 55–75 m/s (at 10-m height) for parts of the Philippines and southern Japan, and Ott proposes a model of extreme wind speeds in the western Pacific (24). Some authors analyze the design codes in the context of tropical cyclones. A study by Jha, et al., sponsored by a Joint Industry Project that included two wind turbine manufacturers (GE Energy and Clipper Wind), compares the reliability levels of an offshore wind turbine designed to IEC 61400-3 and API RP-2A standards operating in several hurricane prone U.S. locations (15, 25, 26). Clausen, et al. (14), recommend increasing the design load safety factor, currently 1.35, to 1.7 in order to maintain the same level of reliability in tropical cyclone areas. Clausen, et al. estimate increasing the safety factor will increase the cost of an onshore turbine 20–30%. The percentage cost increase to strengthen an offshore turbine, like the one we model in this paper, for tropical cyclones is likely to be smaller because a significant portion of the cost of offshore turbines is in the logistics of transporting, installing, and maintaining them.

We have also demonstrated that wind turbines that have external power available to yaw can have a substantially reduced risk of being destroyed. Installing lead-acid batteries to allow a turbine to yaw without external power would add $30,000–$40,000 (2010 prices) to the price of a turbine and 1,400–2,400 kg to its weight, assuming 6 h of backup power for yaw motors that draw 12 kW of power (27). The yaw rate of the turbine we model is 0.3 ° per second. Further work is needed to determine the yaw

rate that is appropriate for hurricanes. Backup power, robust wind direction indicators, and active controls may be a low cost way to reduce risk to the turbine.

A main concern with losing wind turbines during hurricanes is the implication this will have for grid reliability, and more work is needed on this issue. We hypothesize, however, that there is ample warning of hurricanes, and supplemental generation reserves can be brought on line to cover for the wind plants that will be shut down for the months to years that it may take to rebuild buckled towers. However, system operators must make it economical for the owners of such spare generation to stay in business even in years with no hurricane damage, and suitable capacity payment mechanisms will be required.

The probability of hurricane landfalls is not geographically uniform. Fig. 4 plots the offshore wind resources within water shallower than 60 m (2) and the annual rate of hurricane landfalls for states in the eastern United States since 1900 (28). Information for Florida, Alabama, and Mississippi is not included in Fig. 4. Though these states have moderate to high hurricane occurrence rates (0.44, 0.14, and 0.10 y^{-1} respectively), there are no offshore wind resource estimates available for them. The specific results shown in this paper are thus not representative of all the risk of hurricanes to all possible offshore wind farm locations. It is clear, however, that analysis of the type presented here should be performed as part of the wind farm siting analysis.

Our analysis also assumed that historic wind speeds and historic rates of hurricane occurrence are representative of future conditions. Historic conditions may be poor predictors if climate change were to affect hurricane intensity or frequency. Detection of climate change effects on hurricanes is complicated by the very high sensitivity of hurricanes to variations in atmosphere-ocean conditions on multiple time scales, including the multidecadal (29), and by the short period over which hurricane observations are considered reliable (29, 30). Current high-resolution modeling studies project a relatively small increase in Atlantic hurricane intensity with increased global temperatures due to an increase in available thermal energy. Some of these models also identify a possible decrease in Atlantic hurricane frequency, which may be attributable to the stabilization of the upper atmosphere (31). According to these projections, an increase in intensity due to climate change may not be noticeable for the next few decades (30–33). In line with this, Pielke, et al. (6) report that no trends in normalized damages can be detected. On the other hand, a recent observational study (34) finds that there has been an increase in the intensity of the most intense hurricanes. Wind farm developers will invest and operate under the current uncertainties on the future development of Atlantic hurricane activity. The method developed here will support the decision process of wind turbine investors in hurricane-prone areas. Sensitivity analysis on models like the one presented here can allow investors and regulators to see how distribution parameters affect the risk.

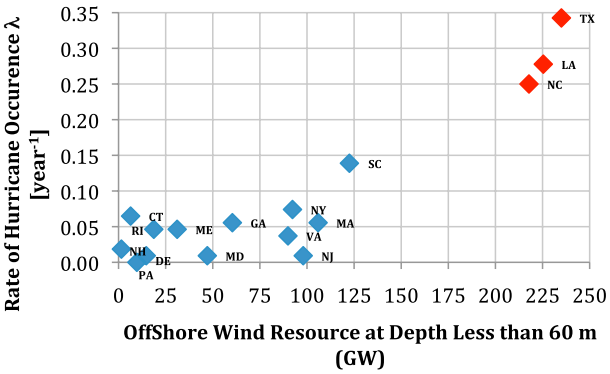

Fig. 4. Resource vs. Hurricane Occurrence Rate λ [$year^{-1}$].

There is a very substantial risk that Category 3 and higher hurricanes can destroy half or more of the turbines at some locations. By knowing the risks before building multiple GW of offshore wind plants, we can avoid precipitous policy decisions after the first big storm buckles a few turbine towers. Reasonable mitigation measures—increasing the design reference wind load, ensuring that the nacelle can be turned into the wind, and building most wind plants in the areas with lower risk—can greatly enhance the probability that offshore wind can help to meet the United States' electricity needs.

Materials and Methods

We model the distribution of the number of wind turbine towers buckled by hurricanes for two cases: (*i*) turbines are not replaced for the life of the wind farm, and (*ii*) turbines are replaced after each hurricane. For each case, we calculate the distributions using two methods: an analytical probability distribution presented here and a Monte Carlo simulation discussed in *SI Text*. All the analyses presented here model a wind farm of 50 NREL 5-MW wind turbines (35) for 20 y. The turbines are shut down with their blades feathered to 90° because hurricane wind speeds are much higher than the maximum operating limit of wind turbines. We believe our results underestimate the probability of loss because we model only buckling of the tower base but ignore damage to other components. Our results may also underestimate the probability of tower buckling because we analyze the onshore version of the NREL 5-MW turbine, which has a rigid foundation structure and is not subjected to wave loads; Jha, et al. (25) develop a more detailed model the NREL 5-MW turbine that includes foundation compliance and wave loads.

Analytical Distribution: Turbine Towers Buckled without Replacement. We model $Y_{\text{no rep}}$, the number of turbine towers that buckle in T-years without replacement as a modified phase-type distribution with six parameters: $Y_{\text{no rep}} \sim \text{PH}(\lambda, \mu, \sigma, \xi, \alpha, \beta)$, where λ is the hurricane occurrence rate; μ, σ, and ξ are the three parameters of the GEV distribution for event maximum wind speed; and α and β are the two parameters of the log-logistic wind speed-turbine buckling probability relationship. We use a phase-type distribution because it models a series of events (storms) that occur randomly with a certain rate, and each buckles an integer number of turbine towers; it gives the distribution for the distribution of time until all towers have been buckled. Fig. 2 plots the results calculated with this method.

Hurricane occurrence is modeled as a Poisson process with rate parameter λ fitted to historical hurricane data. The probability that H, the number of hurricanes that occur in T-years, equals a particular value h is:

$$\Pr(H = h) = \frac{(\lambda T)^h}{h!} e^{-\lambda T}. \quad [1]$$

The maximum 10-min sustained wind speed of each hurricane at 10-m height is modeled as a GEV distribution with a location parameter μ, a scale parameter σ, and a shape parameter ξ fitted to historical hurricane data. The probability density function for W, the maximum sustained wind speed, evaluated at particular value w is:

$$f_W(w) = \frac{1}{\sigma} \exp\left(-\left(1 + \xi \frac{w-u}{\sigma}\right)^{-\frac{1}{\xi}}\right)\left(1 + \xi \frac{w-u}{\sigma}\right)^{-1-\frac{1}{\xi}}. \quad [2]$$

The probability that a single wind turbine tower is buckled by a 10-min sustained hub-height wind speed u is modeled using a log-logistic function with a scale parameter α and a shape parameter β. The parameters for turbines that can and cannot yaw to track wind direction are given in Table 1. These parameters are fit to probabilities of turbine tower buckling calculated by comparing the results of simulations of the 5-MW offshore wind turbine

Table 1. Parameters of log-logistic Functions for Probability of Tower Buckling

	Turbine pointed into wind (Active Yawing)	Turbine pointed perpendicular to wind (Not Yawing)
Damage function parameters (log-logistic function)	$\alpha = 174$, $\beta = 19.3$	$\alpha = 140$, $\beta = 18.6$

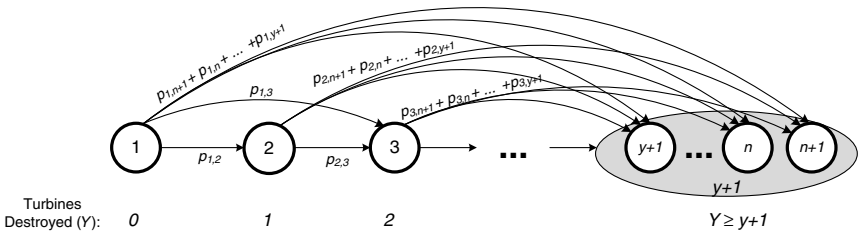

Fig. 5. The Markov Chain used to calculate the probability that the number of turbine towers buckled is less than or equal to y. We define the absorbing state as all the states where $Y_{\text{no rep}} \geq y + 1$.

designed by the NREL (35) to the stochastic resistance to buckling proposed by Sørensen, et al. (36). More extensive details are given in *SI Text*.

The function is fitted to the results of simulations of stresses on a particular turbine design given a yaw direction relative to the wind, a wind TI, and a sustained wind speed u, described in further detail in *SI Text*. The log-logistic function is given by:

$$D(u) = \frac{(u/\alpha)^{\beta}}{1 + (u/\alpha)^{\beta}}. \qquad [3]$$

The number of turbine towers buckled by a single hurricane in a wind farm of n turbines is modeled as a beta-binomial distribution with parameters α_B and β_B. We derive the beta-binomial distribution by fitting a beta distribution with parameters α_B and β_B to the probability of buckling as a function of wind speed weighted by the probability of occurrence of each wind speed (a convolution of D and W) with a nonlinear least-squares fit. The wind speeds W are scaled to turbine hub height using the table of scaling values for hurricanes given by Franklin, et al. (16). Fitting the distribution simplifies the model by replacing the convolution of D and W, which together have five parameters, with a beta distribution that has only two parameters. The beta distribution gives the distribution of buckling probabilities for a single turbine tower given a hurricane with random GEV maximum wind speed. The corresponding beta-binomial distribution with the same parameter values α_B and β_B gives the probability that X, the number of turbine towers that buckle out of n total, equals a particular value x:

$$\Pr(X = x) = \binom{n}{x} \frac{\mathrm{B}(x + \alpha_{\mathrm{B}}, n - x + \beta_{\mathrm{B}})}{\mathrm{B}(\alpha_{\mathrm{B}}, \beta_{\mathrm{B}})}, \qquad [4]$$

where $\mathrm{B}()$ is the beta function.

The cumulative distribution of the number of turbine towers buckled in T or fewer years without replacement, $Y_{\text{no rep}}$, is modeled as a modified phase-type distribution:

$$\Pr(Y_{\text{no rep}} \leq y | \tau \leq T) = \boldsymbol{\pi} \exp(T\mathbf{T}(y,n))\mathbf{e}, \qquad [5]$$

where π is a row vector of initial state probabilities, $\mathbf{T}$ is a matrix of jump intensities for the transitions between states, and $\mathbf{e}$ is a column vector of ones. A phase-type distribution gives the distribution of times τ to reach the absorbing state of a Markov jump process (37, 38). In this application, each jump (state transition) represents a hurricane occurrence, each state represents a unique number or turbines buckled, and the absorbing state is when all n turbine towers in the wind farm have buckled. We modify the phase-type distribution to calculate the distribution of the number of turbine towers buckled $Y_{\text{no rep}}$ in a fixed time T by iteratively redefining the absorbing state to include cases where less than n turbine towers are bucked, as shown in Fig. 5.

This redefinition of the absorbing state makes the sizes of the vectors π and $\mathbf{e}$ a function of y and makes both the size and values of the matrix $\mathbf{T}$ a function of y. To calculate the probability that y or fewer turbine towers buckle, we define the absorbing state to include an integer number of turbine towers buckled from $y + 1$ to n. There are $y + 1$ total states; the $y + 1^{\text{st}}$ state is the absorbing state. The term π in **[5]** is a $y + 1$ element row vector of initial state probabilities; in this application $\pi = [1\ 0 \ldots 0]$ because the distribution begins in state 1 (no turbine towers buckled). The term $\mathbf{e}$ is a column vector of ones: $[1\ 1 \ldots 1]^T$. The term $\mathbf{T}$ is a $(y + 1) \times (y + 1)$ matrix of jump intensities, where the jump intensity $\mathbf{T}_{ij}(y,n)$ from the i th state to the j th state is the product of λ, the rate of hurricane occurrence, and p_{ij}, the probability a hurricane causing a transition from state i to state j by buckling turbine towers. The off-diagonal elements of $\mathbf{T}(y,n)$ in the i th row and j th are calculated by:

$$T_{ij}(y,n) = \lambda\ \text{beta-binomial}(n - i + 1, n - j + 1; \alpha_B, \beta_B) \qquad j \geq i \qquad [6]$$

and the diagonal elements are calculated by:

$$T_{ii}(y,n) = -\left(t_i(y,n) + \sum_{j>i} T_{ij}(y,n)\right), \qquad [7]$$

where $\mathbf{t}$ is the jump intensity for a hurricane that jumps directly to the absorbing state (i.e., destroys all remaining turbines):

$$t_i(y,n) = \lambda \sum_{m=0}^{n-y-1} \text{beta-binomial}(n, n - m; \alpha_B, \beta_B). \qquad [8]$$

The off-diagonal elements of $\mathbf{T}$ do not sum to 1 along a row because some hurricanes do not cause a state transition (i.e., some hurricanes do not buckle any turbine towers).

Analytical Distribution: Turbine Towers Buckled with Replacement. We model Y_{rep}, the number of turbine towers that buckle in T-years with replacement as a compound Poisson distribution with six parameters: $Y_{\text{rep}} \sim$ Compound Possion (λ, μ, σ, ξ, α, β). We use a compound Poisson distribution because it models the distribution of the sum of independent identically distributed events (hurricanes buckling wind turbines, in this case) that occur as a Poisson process. The compound Poisson distribution is a convolution of the Poisson distribution given in **[1]** for the number of hurricanes that occur in T-years and the beta-binomial distribution given in **[4]** for number of turbine towers buckled by each hurricane. No analytical expression exists for the PDF (probability density function) or CDF (cumulative distribution function) of a compound Poisson distribution that contains a beta-binomial distribution. We use Panjer's recursion (39, 40), an iterative method, to approximate the PDF. The details are given in *SI Text*.

Table 2. Distribution Parameters for Poisson and GEV Distributions

	Rate of hurricane occurrence [events/year]	Max. sustained hurricane wind speed: GEV distribution [knots]	Geographic range of hurricanes modeled (lat/long)
Galveston County, TX	$\lambda = 0.19$	$\mu = 78.7$, $\sigma = 12.1$, $\xi = 0.251$	25.5°N–30°N 92°W–99°W
Dare County, NC	$\lambda = 0.21$	$\mu = 77.6$, $\sigma = 11.9$, $\xi = -0.0366$	32°–36.5°N 71°–81°W
Atlantic County, NJ	$\lambda = 0.047$	$\mu = 77.2$, $\sigma = 10.6$, $\xi = -0.0544$	36°–41°N 71°–77.5°W
Dukes County, MA	$\lambda = 0.075$	$\mu = 73.2$, $\sigma = 6.99$, $\xi = -0.139$	40.3°–42°N 66°–74.5°W

Application to Specific Locations. The rate of hurricane occurrence parameter λ for the Poisson distribution given in **[1]** is calculated as the number of hurricanes to make landfall (direct and indirect strikes) in each county between 1900 and 2007 (17), divided by the length of the time period. The calculated values for the locations we investigate are given in Table 2. The parameters for the GEV distribution given in **[2]** are fit to historical data for the maximum 10-min sustained wind speed at 10-m height for all hurricanes to pass through the geographic ranges of interest (described in the fourth column of Table 2) between 1851 and 2008.

ACKNOWLEDGMENTS. This work was supported in part by the Carnegie Mellon Electricity Industry Center, the U.S. Environmental Protection Agency (EPA) STAR (Science to Achieve Results) fellowship program, the Doris Duke Charitable Foundation, the Richard King Mellon Foundation, the Heinz Endowments, the Department of Energy National Energy Technology Laboratory, and the Electric Power Research Institute through the RenewElec project at Carnegie Mellon University. Support was also received from the Center for Climate and Energy Decision Making created through a cooperative agreement between the National Science Foundation (SES-0949710) and Carnegie Mellon University.

1. DOE (2010) *Electric Power Annual* (Energy Information Administration, Washington DC), Department of Energy.
2. Shwartz M, Heimiller D, Haymes S, Musial W (2010) Assessment of Offshore Wind Energy Resources for the United States. (National Renewable Energy Laboratory, Golden, CO).
3. Lindenberg S, Smith B, O'Dell K, DeMeo E, Ram B (2008) *20% Wind Energy by 2020: Increasing Wind Energy's Contribution to US. Electricity Supply* (National Renewable Energy Laboratory, Golden, CO).
4. Blake E, Rappaport E, Landsea CW (2007) The Deadliest, Costliest, and Most Intense United States Tropical Cyclones from 1851 to 2006; NOAA Technical Memorandum NWS TPC-5. (National Hurricane Center, FL).
5. Changon S (2009) Characteristics of severe Atlantic hurricanes in the United States 1949-2006. *Natural Hazards* 48:329–337.
6. Pielke R, et al. (2008) Normalized hurricane damage in the United States. *Natural Hazards Reviews* 2008:29–42.
7. Landsea CW, Pielke RA, Mestas-Nuñez AM, Knaff JA (1999) Atlantic Basin hurricanes: indices of climate change. *Climatic Change* 42:89–129.
8. Goldenberg SB, Landsea CW, Mestas-Nunez AM, Gray WM (2001) The recent increase in Atlantic hurricane activity: causes and implications. *Science* 293:474–479.
9. Cruz A, Krausmann E (2008) Damage to offshore oil and gas facilities following hurricanes Katrina and Rita: an overview. *J Loss Prevent Proc* 21(6):620–626.
10. Liu H, Davidson R (2007) Statistical forecasting of electric power restoration times in hurricanes and ice storms. *Power Syst* 22:2270–2279.
11. DOE (2005) *Company Plans Large Wind Plant Offshore of Galveston* (Energy Efficinecy & Renewable Energy Network News, Washington, DC).
12. DOE (2010) *Interior Department Signs First U.S. Offshore Wind Energy Lease* (Energy Efficinecy & Renewable Energy Network News, Washington, DC).
13. Takahara K, et al. (2004) *Damages of wind turbine on Miyakojima Island by Typhoon Maemi in 2003*.
14. Clausen N, et al. (2007) Wind farms in regions exposed to tropical cyclones. (Germanischer Lloyd WindEnergie GmbH, Hamburg) European Wind Energy Conference and Exhibition.
15. IEC IEC, Wind Turbines- Part 3: Design requirements for offshore wind turbines (Geneva) IEC 61400-3..
16. Franklin J, Black M, Valde K (2003) GPS dropwindsonde wind profiles in hurricanes and their operational implications. *Weather and Forecasting* 18:32–44.
17. National-Hurricane-Center (2010) County by county hurricane strikes 1900–2009. (National Hurricane Center, Coral Gables, FL), p 154 Updated from Jarrell JD, Hebert PJ, Mayfield M 1992: "Hurricane Experience Levels of Coastal County Populations from Texas to Maine" NOAA Technical Memorandum NWS NHC-46 .
18. Schroeder J, Smith D, Peterson R (1998) Variation of turbulence intensities and integral scales during the passage of a hurricane. *J Wind Eng Ind Aerod* 77:65–72.
19. Jarvinen BR (2006) Storm tides in twelve tropical cyclones (including four intense New England hurricanes). (National Hurricane Center, FL) p 99.
20. Bossak BH (2003) Early 19th Century U S. Hurricanes: A GIS Tool and Climate Analysis. (Florida State University, Tallahassee, FL), PhD dissertation.
21. Argyriadis K (2003) Recommendations for Design of Offshore Wind Turbines (RECOFF), Section 2.1: External Conditions.
22. Garciano L, Koike T (2010) New reference wind speed for wind turbines in typhoon-prone areas in the Philippines. *J Struct Eng* 136:463–467.
23. Clausen N-E, Ott S, Tarp-Johansen N-J, Nørgård P, Larsén XG (2006) Design of wind turbines in an area with tropical cyclones. (European Wind Energy Conference and Exhibition, Athens), pp 1–10.
24. Ott S (2006) Extreme winds in the western North Pacific. pp 1–39 Riso-R-1544(EN) Riso National Laboratory, Roskilde, Denmark.
25. Jha A, Dolar D, Musial W, Smith C (May 2010) On hurricane risk to offshore wind turbines in US waters. *Presented at the Offshore Technology Conference* (2010 Offshore Technology Conference, Houston, TX), pp 3–6.
26. API (2000) Recommended Practice for Planning, Designing, and Constructing Fixed Offshore Platforms—Working Stress Design. 1st Ed (American Petroleum Institute, Washington, DC).
27. Aabakken J (2006) *Power Technologies Energy Data Book* (National Renewable Energy Laboratory, Golden, CO), 4th Ed.
28. Jarvinen BR, Neumann CJ, Davis MAS (1988) A Tropical Cyclone Data Tape for the North Atlantic Basin, 1886-1983: Contents, Limitations, and Uses. *NOAA Tech. Memo NWS NHC 22* (National Hurricane Center, FL), 1984, updated 1988.
29. Grossmann I, Morgan MG (2011) Tropical cyclones, climate change, and scientific uncertainty: What do we know, what does it mean, what should be done? *Climatic Change* 110:543–579.
30. Landsea CW, Harper BA, Hoarau K, Knaff JA (2006) Can we detect trends in extreme tropical cyclones? *Science* 313:452–454.
31. Knutson TR, et al. (2010) Tropical cyclones and climate change. *Nat Geosci* 3:157–163.
32. Bengtsson L, et al. (2007) How may tropical cyclones change in a warmer climate? *Tellus A* 59:539–561.
33. Bender MA, et al. (2010) Modeled impact of anthropogenic warming of the frequency of intense Atlantic hurricanes. *Science* 327:454–458.
34. Elsner JB, Kossin JP, Jagger TH (2008) The increasing intensity of the strongest tropical cyclones. *Nature* 444:92–95.
35. Jonkman J, Butterfield S, Musial W, Scott G (2009) *Definition of a 5-MW Reference Wind Turbine for Off-shore System Development* (National Renewable Energy Laboratory, CO).
36. Sørensen J, Tarp-Johansen N (2005) Reliability-based optimization and optimal reliability level of offshore wind turbines. *Int J Offshore Polar* 15:141–146.
37. Neuts MF (1995) *Matrix-Geometric Solutions in Stochastic Models: An Algorithmic Approach* (Johns Hopkins University Press, MD).
38. Bladt M (2005) A review on phase-type distributions and their use in risk theory. *ASTIN Bull* 35:145–161.
39. Panjer H (1981) Recursive evaluation of a family of compound distributions. *ASTIN Bull* 12:22–26.
40. Dickson D (1995) A review of Panjer's Recursion formula and its applications. *British Actuarial Journal* 1:107–124.

Supporting Information

Rose et al. 10.1073/pnas.1211977109

Supporting Information corrected July 19, 2012

SI Text

Risk from Multiple Hurricanes with Replacement. In the main text, Fig. 2 present cumulative distribution function (CDF) plots for the number of turbines destroyed in 20 y if buckled turbine towers are not replaced. Here we present similar results for the case in which buckled towers are replaced after each storm. Fig. S1 plots the CDF for each location for two cases: turbines that can yaw to track wind direction (dashed lines) and turbines that cannot yaw (solid lines).

In this scenario, buckled towers are replaced after each storm so there is no limit to the maximum number of towers that buckle. There is a 10% probability that more than 50 turbine towers will buckle in Galveston County and a 1% probability that more than 50 will buckle in Dare County.

Risk from Multiple Hurricanes, Category 4 and 5 Hurricanes Excluded. To illustrate the effect of excluding Category 4 and 5 hurricanes for Dare, Atlantic, and Dukes counties, we plot the CDF of the number of turbines damaged with and without those higher-category hurricanes. The results for the case that turbines cannot yaw to track the wind direction are shown in Fig. S2, where solid lines plot the results for all hurricanes and dotted lines plot the results excluding Category 4 and 5 hurricanes. Similarly, the results for the case that turbines can actively yaw are shown in Fig. S3, where solid lines plot the results for all hurricanes and dotted lines plot the results excluding Category 4 and 5 hurricanes.

Analytical Distribution: Turbine Towers Buckled with Replacement. As described in the main text, we use a compound Poisson distribution to model Y_{rep}, the total number of turbine towers buckled in T-years in a wind farm of n turbines if towers are immediately replaced after they are buckled by a hurricane. The compound Poisson distribution is a function of six parameters: λT, μ, σ, ξ, α, and β.

$$Y_{\text{rep}} \sim \text{compound Poisson}(\lambda T, \mu, \sigma, \xi, \alpha, \beta). \quad \textbf{[S1]}$$

No analytical expression exists for the PDF (probability density function) or CDF of a compound Poisson distribution that contains a beta-binomial distribution. We use Panjer's recursion (1, 2), an iterative method, to compute the exact pdf:

$$\Pr(Y_{\text{rep}} = y) = g_y = \sum_{j=1}^{y} \left(a + \frac{bj}{y}\right) f_i g_{y-j}, \quad \textbf{[S2]}$$

where

$$f_j = \begin{cases} \Pr(X_i = j) & j \le n \\ 0 & j > n \end{cases}. \quad \textbf{[S3]}$$

The value of f_j is zero for $j > n$ in Eq. **S2** because the beta-binomial distribution for the number of turbine towers buckled in the i th hurricane X_i is not defined for $x > n$; i.e, the number of towers buckled in one hurricane cannot be larger than the number of turbines in the wind farm.

Panjer defines a and b for a Poisson distribution (1):

$$a = 0$$

$$b = \lambda T.$$

The initial value of f is:

$$f_0 = \Pr(X_i = 0) = \binom{n}{0} \frac{\mathrm{B}(0 + \alpha_B, n - 0 + \beta_B)}{\mathrm{B}(\alpha_B, \beta_B)} = \frac{\mathrm{B}(\alpha_B, n + \beta_B)}{\mathrm{B}(\alpha_B, \beta_B)} \quad \textbf{[S4]}$$

and the initial value g_0, from (3), gives the probability that no turbine towers are buckled by hurricanes in T-years as the probability that no hurricanes occur ($H = 0$) plus the probability that a positive number of hurricanes occur but cause no damage:

$$\begin{aligned} g_0 &= \Pr(H = 0) + \Pr(Y = 0 | H > 0) \\ &= \frac{(\lambda T)^0}{0!} e^{-\lambda T} + \sum_{i=1}^{\infty} \Pr(X = 0) \Pr(H = i) \\ &= e^{-\lambda T} + \sum_{i=1}^{\infty} \left(\binom{n}{0} \frac{\mathrm{B}(0 + \alpha_B, n - 0 + \beta_B)}{\mathrm{B}(\alpha_B, \beta_B)} \right)^i \frac{(\lambda T)^i}{i!} e^{-\lambda T} \\ &= e^{-\lambda T} + \sum_{i=1}^{\infty} \left(\frac{\mathrm{B}(\alpha_B, n + \beta_B)}{\mathrm{B}(\alpha_B, \beta_B)} \right)^i \frac{(\lambda T)^i}{i!} e^{-\lambda T}, \end{aligned} \quad \textbf{[S5]}$$

where $\mathrm{B}(\alpha, \beta)$ is the beta function:

$$\mathrm{B}(\alpha_B, \beta_B) = \frac{\Gamma(\alpha_B)\Gamma(\beta_B)}{\Gamma(\alpha_B + \beta_B)} = \frac{(\alpha_B - 1)!(\beta_B - 1)!}{(\alpha_B + \beta_B - 1)!} \quad \textbf{[S6]}$$

and $\Gamma()$ is the Gamma function.

Monte Carlo Distribution: Turbine Towers Buckled with Replacement. To check the compound Poisson distribution described above, we use Monte Carlo simulations to calculate Y_{rep}, the distribution of the total number of turbine towers buckled in T-years in a wind farm of n turbines if towers are replaced after each hurricane. We simulate 10,000 20-y periods using the same distributions used in the compound Poisson distribution: H for the frequency of hurricane occurrence, W for the maximum sustained wind speed, and D for the probability of buckling as a function of wind speed.

For each simulated 20-y period in a given location, we calculate the total number of towers that buckle according to the following procedure:

1. Draw number of hurricanes from Poisson distribution H described in *Hurricane Frequency*.
2. Draw maximum sustained wind speed for each hurricane from Generalized Extreme Value (GEV) distribution W described in *Hurricane Intensity* (W).
3. Scale maximum sustained wind speed to hub height (4) and calculate probability of a single turbine tower buckling at that wind speed using the log-logistic damage function described in *Wind Turbine Damage Function* (D).
4. Calculate the number of towers buckled in each hurricane using a Binomial distribution with the probability of buckling calculated in step 3 and n turbines.

A comparison of the distributions calculated with the compound Poisson distribution and the Monte Carlo simulation is shown in Fig. S4.

Monte Carlo Distribution: Turbine Towers Buckled without Replacement. To check the phase-type distribution described in the main text, we use Monte Carlo simulations to calculate $Y_{\text{no rep}}$, the distribution of the total number of turbine towers buckled in T-years in a wind farm of n turbines if turbines are not replaced after they are destroyed. We simulate 10,000 20-y periods using the same distributions used in the phase-type distribution: H for the frequency of hurricane occurrence, W for the maximum sustained wind speed, and D for the probability of buckling as a function of wind speed.

For each simulated 20-y period in a given location, we calculate the total number of turbine towers buckled according to the following procedure:

1. Draw number of hurricanes from Poisson distribution H described in *Hurricane Frequency*.
2. Draw maximum sustained wind speed for each hurricane from GEV distribution W described in *Hurricane Intensity* (W).
3. Scale maximum sustained wind speed to hub height (4) and calculate probability of a single turbine tower buckling at that wind speed using the log-logistic damage function described in *Wind Turbine Damage Function* (D).
4. Calculate the number of remaining turbines buckled in each hurricane using a Binomial distribution with the probability of buckling calculated in step 3 and the number of turbines remaining after all the previous hurricanes.

A comparison of the distributions calculated with the phase-type distribution given in the main text and the Monte Carlo simulation described above is shown in Fig. S5.

Hurricane Frequency (H). We fit a Poisson distribution to the rate of hurricane occurrence in a particular county by dividing the number of hurricanes to make landfall in that county from 1900 to 2006 by the number of years (5). Table 2 in the main text lists the resulting rate of hurricane occurrence values λ for the four counties we examine. This method of calculating the rate of hurricane occurrence assumes that the rate is constant and equal to the average rate. However, previous research has shown strong associations between North Atlantic hurricane activity and atmosphere-ocean variability on different time scales, including the multidecadal (6, 7).

Hurricane Intensity (W). We fit a GEV distribution to the maximum 10-min sustained wind speed at 10-m height of hurricanes that pass through a region around the counties we examine. Table 2 in the main text gives the parameters of the fitted GEV distributions for each location and the latitude and longitude limits of the regions around those locations. Fig. 6 compares the empirical and fitted CDFs for the maximum sustained wind speed at each location.

Wind Turbine Damage Function (D). We fit a log-logistic distribution to the probability of a wind turbine tower buckling as a function of 10-min sustained wind speed at hub height. The probability of the turbine tower buckling at a given wind speed is calculated by simulating tower bending moments of a 5-MW National Renewable Energy Laboratory (NREL) turbine and comparing them to the stochastic resistance to buckling of the turbine tower. In our analysis, we model the 5-MW wind turbine design created by the NREL for two load cases (active yawing and not yawing).

We calculate separate damage functions for the "active-yawing" and "not-yawing" load cases because those are the best and worst case wind load conditions for an idling wind turbine. The active-yawing case assumes the grid power is available to the turbine or the turbine has a backup power source for the yaw motors and control system; the not-yawing case assumes the turbine does not have a backup power source and grid power has been lost, a typical occurrence in hurricanes (8). The current design standards for wind turbines given by the IEC (9) and Germanischer-Lloyd (10) require that an idling wind turbine be able to survive 10-min sustained wind with 50-y recurrence period (load case 6.2). If backup power is not available for the yaw and control systems, the IEC standard requires the turbine must be able to survive a yaw misalignment of $\pm 180°$ and the Germanischer-Lloyd standard specifies $\pm 30°$. The active-yawing case we simulate assumes backup power for the yaw system, and the not-yawing case assumes a yaw misalignment of 90°. The probability of buckling as a function of wind speed for the active-yawing and not-yawing cases are plotted in Fig. S7.

Bending Moment Simulation. We calculate a range of maximum tower bending moments by simulating the mechanical loads on an NREL 5-MW turbine (11) for mean wind speeds from 40 to 110 m/s (78–214 knots) at hub height. We simulate 30 10-min periods for each mean wind speed, with the turbulence intensity (TI) of each period drawn from a lognormal distribution with a mean of 9% and standard deviation of 1.5%. The turbine is shut down with blades feathered because the wind speed is higher than the operating limit.

The NREL 5-MW turbine we simulate is designed for offshore installation in an IEC Class 1B wind regime (12). We simulate the configuration referred to by NREL as "onshore,"which is identical to the "offshore" except that the onshore configuration assumes a rigid foundation and no ocean wave loads. The rigid foundation we use in our simulations is likely to give lower estimates of the maximum tower bending moment than a compliant offshore foundation design, according to simulations conducted by Bush, et al. (13). Neglecting wave loads is also likely to give lower estimates of the maximum tower bending moment because wave loads contribute significantly to the tower bending moment, as shown by simulations conducted by Jha, et al. (14). These two simplifications of the turbine model embodied in the onshore configuration likely underestimate tower bending moments and therefore underestimate the probabilities of tower buckling.

We use the TurbSim software, version 1.50 (15), to simulate a turbulent 3D wind field. We generate 30 10-min wind speed time series for each mean wind speeds from 40–110 m/s (78–214 knots) in 2 m/s increments. The turbulence around each mean wind speed is generated from the Normal Turbulence Model given in the IEC 61400-3 design standard (9). For each simulation, we randomly draw a 10-min TI value from a lognormal distribution with a mean of 9% and a standard deviation of 1.5%. TI is calculated as the quotient of the 10-min mean wind speed u and the 10-min standard deviation σ : $\text{TI} = u_{10\,\text{min}}/\sigma_{10\,\text{min}}$. The lognormal distribution is fitted to TI values measured in hurricanes and tropical cyclones over water. The directly measured TI values are given in Table S1 and TI values calculated from directly measured gust factors (GF) are given in Table S2. TI values are calculated from measured GF values according to the relationship $\text{TI} = (\text{GF} - 1)/\alpha$, where $\alpha = 2.44$ is averaged from several values given by Yu, et al. (16). GF values given by Vickery, et al. use a 60-min averaging period; Vickery, et al. recommend dividing the GF by 1.055 to calculate the 10-min value (17). We scale the TI values to hub height $h = 90$ meters using the following relationship derived from equation 2.3.2-3 in the API RP-2A design standard:

$$\text{TI}(h) = \text{TI}(h_{\text{ref}})\left(\frac{h}{h_{\text{ref}}}\right)^{-0.22}. \qquad \text{[S7]}$$

Fig. S8 plots the TI values directly measured and derived from GF measurements in tropical cyclones, other TI values measured

over water in extratropical storms, the tropical-cyclone TI values scaled to hub height, and the power-law from Eq. **S7** used to scale them to hub height.

The bending moment on base of the turbine tower is dominated by three forces: aerodynamic force on the turbine blades, aerodynamic force on the nacelle, and aerodynamic force on the tower. We calculate the horizontal components (x and y) of the moments caused by those three forces for each 0.0125-s time step in a 10-min simulation. We select the maximum vector sum of the moments after excluding the first 60-s of the simulation to remove transient oscillations caused by initial conditions of the simulation. The process is repeated for 30 simulations at each value of mean wind speed. Fig. S9 plots the magnitude of the average of maximum tower bending moments as a function of mean wind speed, with the contributions of wind loads on the blades, nacelle, and tower separated. Fig. S9*A* plots the moments for the "Active-Yawing" load case, where the wind strikes the turbine head-on, and Fig. S9*B* plots the moments for the "Not-Yawing" load case, where the wind strikes the turbine from the side.

We simulate the moment caused by the aerodynamic force on the feathered blades using the NREL FAST software, version 7.00.01a-bjj (18). The output signals for the x- and y-components of the bending moment at the tower base are labeled "TwrBsMxt" and "TwrBsMyt." The maximum moments in some simulations are anomalous, especially for the Not-Yawing load case where the wind strikes the turbine from the side. We believe these outliers are the result of numerical convergence problems in the FAST software. We exclude the outliers by fitting a robust quadratic least-squares line with bisquare weights to the maximum moments as a function of mean wind speed and excluding maximum moments outside the ±50% range around the quadratic regression line, as shown in Fig. S10.

FAST does not simulate wind loads on the nacelle or tower (19, 20), so we calculate the moment caused by the aerodynamic force on the nacelle using the following expression adapted from sections 5.2.1 and 5.3.1 of the DNV-RP-C205 design standard (21):

$$M_{\text{nacelle}} = \begin{cases} C_{\text{front}}(\frac{1}{2}\rho_a u_x^2) S_{\text{front}} h_{\max}\hat{x} + C_{\text{side}}(\frac{1}{2}\rho_a u_y^2) S_{\text{side}} h_{\max}\hat{y} & \text{Active yaw tracking} \\ C_{\text{side}}(\frac{1}{2}\rho_a u_x^2) S_{\text{side}} h_{\max}\hat{x} + C_{\text{front}}(\frac{1}{2}\rho_a u_y^2) S_{\text{front}} h_{\max}\hat{y} & \text{No yaw tracking} \end{cases}, \quad \textbf{[S8]}$$

where u_x and u_y are the horizontal components of wind speed parallel to and perpendicular to the long axis of the nacelle and $\hat{x}$ and $\hat{y}$ are the unit vectors in those directions. The surface area S and shape coefficient C of the nacelle are based on the nacelle dimensions of the comparable REpower 5M offshore turbine, which is 6 m wide, 6 m tall, and 18 m long (22). The shape factors are taken from Table 5-5 in the DNV-RP-C205 design standard (21). The parameter values are given in Table S3.

The bending moment caused by wind load on the tower is more complicated because the wind acts across the whole length of the tower and because the diameter of the tower decreases with height. We model the diameter of the tower D as a function of height h as a linear function:

$$D(h) = D_{\text{base}} + \left(\frac{D_{\text{top}} - D_{\text{base}}}{h_{\max}}\right)h, \quad \textbf{[S9]}$$

where D_{base} is the tower diameter at its base, D_{top} is the diameter at the top, and $h_{\max}$ is the height of the top of the tower. The shape coefficient for the tower, a long cylinder, is $C_{\text{tower}} = 0.5$ from Fig. 6-6 in the DNV-RP-C205 design standard (21). Assuming a uniform wind speed across the whole length of the tower, the bending moment from the wind load on the tower is:

$$\begin{aligned} M_{\text{tower}} &= C_{\text{tower}}\left(\frac{1}{2}\rho_a u^2\right)\int_0^{h_{\max}}\left(D_{\text{base}} + \frac{D_{\text{top}} - D_{\text{base}}}{h_{\max}}\right)h\,dh \\ &= \frac{1}{6}C_{\text{tower}}\left(\frac{1}{2}\rho_a u^2\right)h_{\max}^2(D_{\text{base}} + 2D_{\text{top}}). \end{aligned} \quad \textbf{[S10]}$$

The contribution of the wind load on the tower is significant, especially at higher wind speeds, as shown in Fig. S9.

Calculation of Buckling Probability. Given the magnitude M of the maximum tower bending moments calculated above, we calculate the probability of a turbine tower buckling by comparing the magnitude of the simulated bending moments to a random variable for the resistance of a tower to buckling.

For each load case (Active-Yawing or Not-Yawing) and mean wind speed u, we create 5,000 bending moment values by repeatedly sampling the simulation results with equal probability. If no anomalous values were excluded, there are 30 simulation values to sample from; there are fewer if some were excluded.

We calculate 5,000 resistance to buckling values M_{cr} according to Eq. **S11**, the resistance to buckling of a thin-walled cylinder, by randomly sampling the parameters from the distributions given in Table S4 (23):

$$M_{\text{cr}} = \frac{1}{6}\left(1 - 0.84\frac{D}{t}\frac{X_{y,ss}F_y}{X_{E,ss}E}\right)(D^3 - (D-2t)^3)X_{y,ss}X_{\text{cr}}F_y. \quad \textbf{[S11]}$$

The damage function D at a given 10-min mean wind speed for a given load case (Active-Yawing or Not-Yawing) is calculated by comparing all the sampled bending moment values to the sampled resistance-to-buckling values to find the probability of buckling for each 10-min mean wind speed u:

$$D(u) = \Pr(M_{\text{cr}} \le M(u)) \quad \textbf{[S12]}$$

We generalize the results calculated in Eq. **S12** by fitting a log-logistic function to the data. The form of the log-logistic function is given by Eq. **3** in the paper.

The distribution of number of turbine towers buckled in a hurricane is modeled in [**4**] (from the main text) by a beta-binomial distribution. The beta-binomial distribution gives a binomial distribution for the number of turbine towers buckled in a single hurricane, where all turbines have the same probability of buckling. The assumption that all turbines have the same buckling probability implies a strong correlation between the buckling of the towers in the wind farm. Our results are not sensitive to this assumption of strong correlation. Fig. S11 compares the distribution of the number of turbine towers buckled in a single hurricane for two different models of correlation between tower buckling. The model labeled "Identical turbines" in Fig. S11 is the model we use in our paper, where the number of towers buckled is binomial distributed and all turbines have the same probability of buckling. We compare that model to a model that implies a weaker correlation between turbines, labeled "Distribution of turbine properties." In that distribution, each turbine is exposed to different wind conditions with turbulence intensities drawn from a lognormal distribution and each tower has a different resistance to buckling calculated with [**S11**]. The results in Fig. S11 are calculated for a mean wind speed of 70 m/s

(136 knots) but results for other mean wind speeds show similarly good matches between the distributions.

Nomenclature. T = time period to investigate
n = number of turbines in the wind farm
u = 10-min average hub height wind speed
λ = rate parameter for occurrence of hurricanes
μ = location parameter for distribution of wind speed in a hurricane
σ = scale parameter for distribution of wind speed in a hurricane
ξ = shape parameter for distribution of wind speed in a hurricane
α = scale parameter for the log-logistic distribution of the probability of a turbine tower buckling at a 10-min average wind speed u
β = shape parameter for the log-logistic distribution of the probability of a turbine tower buckling at a 10-min average wind speed u
α_B, β_B = parameters of the beta-binomial distribution for the distribution of turbine towers buckled in a single hurricane (parameters are derived by fitting a beta distribution to the damage function weighted by the probability of occurrence of wind speed)
W = random variable for the maximum sustained (10-min) wind speed of a hurricane
w = a wind speed drawn from W
D = random variable for the probability of turbine damage for a given wind speed w
d = a damage probability drawn from D
X = random variable for the number of turbines damaged in one hurricane
x = a number of damaged turbines drawn from X
H = random variable for the number of hurricanes in T-years
h = a number of hurricanes drawn from H
Y_{rep} = random variable for the number of turbines damaged in T-years with replacement
$Y_{\text{no rep}}$ = random variable for the number of turbines damaged in T-years no replacement
y = a number of turbines damaged drawn from Y
a = constant for alternative description of the Poisson distribution used in Panjer recursion from (24)
b = constant for alternative description of the Poisson distribution used in Panjer recursion from (24)
$\mathbf{T}$ = transition matrix for phase-type distributions
τ = the time to destroy all turbines (or reach an absorbing state) if turbines are not replaced
z = number of Monte Carlo simulations
$\mathbf{T}$ = matrix of state transition intensities. The values T_{ij} are the probabilities of transition from state i to state j. There are $n+1$ states, where the $n+1$ state is the absorbing state
$\mathbf{t}$ = vector of intensities of state transitions directly to the absorbing state
π = starting probabilities for each state
k = number of turbines in absorbing state
m = an index for summation
C = shape coefficient
ρ_a = density of dry air at 20 °C
u = wind speed
S = surface area

1. Panjer H (1981) Recursive evaluation of a family of compound distributions. *ASTIN Bulletin* 12:22–26.
2. Dickson D (1995) A review of Panjer's recursion formula and its applications. *British Actuarial Journal* 1:107–124.
3. Mikosch T (2009) *NonLife Insurance Mathematics: An Introduction with the Poisson Process* (Springer, Berlin) 2nd Edition Ed.
4. Franklin J, Black M, Valde K (2003) GPS dropwindsonde wind profiles in hurricanes and their operational implications. *Weather and Forecasting* 18:32–44.
5. National-Hurricane-Center (2010) County by county hurricane strikes 1900–2009. Updated from Jarrell, JD, Hebert PJ, and Mayfield M 1992: "Hurricane experience levels of coastal county populations from Texas to Maine" *NOAA Technical Memorandum NWS NHC-46* (Coral Gables, FL) pp 154.
6. Landsea CW, Pielke RA, Mestas-Nuñez AM, Knaff JA (1999) Atlantic Basin hurricanes: indices of climate change. *Climatic Change* 42:89–129.
7. Goldenberg SB, Landsea CW, Mestas-Nuñez AM, Gray WM (2001) The recent increase in Atlantic hurricane activity: causes and implications. *Science* 293:474–479.
8. Liu Y, Singh C (2011) A methodology for evaluation of hurricane impact on composite power system reliability. *IEEE Transactions on Power Systems* 26(1):145–152.
9. IEC (2009) *International Electrotechnical Commission, Wind Turbines- Part 3: Design requirements for offshore wind turbines* (IEC, Geneva) IEC 61400-3 First Ed.
10. Germanischer-Lloyd-Industrial-Services (2005) *Guideline for the Certification of Offshore Wind Turbines* (Germanischer Lloyd Industrail Services, Hamburg), pp 4-34 to 4-41.
11. Jonkman J, Butterfield S, Musial W, Scott G (2009) *Definition of a 5-MW Reference Wind Turbine for off-shore system development*. (National Renewable Energy Laboratory, CO).
12. Jonkman JM, Buhl ML, Jr. (2007) Loads analysis of a floating offshore wind trubine usin fully coupled simulation. *WindPower Conference & Exhibition* (National Renewable Energy Laboratory, CO).
13. Bush E, Manuel L (2009) Foundation models for offshore wind turbines. *47th Aerospace Sciences Meeting* (American Institute of Aeronautics and Astronautics, VA).
14. Jha A, Dolar D, Musial W, Smith C (2010) On hurricane risk to offshore wind turbines in US waters. *Presented at the Offshore Technology Conference* (MMI Engineering, Oakland, CA).
15. Jonkman B (2009) TurbSim User's Guide: Version 1.50.1-85. (National Renewable Energy Laboratory, Golden, CO).
16. Yu B, Gan Chowdhury A (2009) Gust factors and turbulence intensities for the tropical-cyclone environment. *Journal of Applied Meteorology and Climatology* 48:534–552.
17. Vickery PJ, Skerlj PF (2005) Hurricane gust factors revisited. *Journal of Structural Engineering* 131:825–832.
18. Jonkman J (2005) FAST User's Guide.1-143. (National Renewable Energy Laboratory, Golden, CO).
19. Jonkman J (2011) Normal aerodynamic forces on the tower. (wind.nrel.gov/forum/wind/. Retrieved November 4, 2011 from https://wind.nrel.gov/forum/wind/viewtopic.php?f=16&t=493).
20. MMI Engineering (2009) *Comparative Study of OWTG Standards* (MMI Engineering, Oakland, CA), pp 1–197.
21. DNV (2010) *Recommended Practice DNV-RP-C205: Environmental Conditions and Environmental Loads* (Det Norske Veritas, Oslo), pp 1–122.
22. de Vries E (2009) REpower Systems: less is more offshore. (RenewableEnergyWorld.com. Brunsbuttel, Germany. Retrieved October 25, 2011 from http://www.renewableenergyworld.com/rea/news/article/2009/04/repower-systems-less-is-more-offshore.
23. Sørensen J, Tarp-Johansen N (2005) Reliability-based optimization and optimal reliability level of offshore wind turbines. *International Journal of Offshore and Polar Engineering* 15:141–146.
24. Sundt B, Jewell W (1981) Further results on recursive evaluation of compound distributions. *ASTIN Bulletin* 12:27–39.
25. Paulsen BM, Schroeder JL (2005) An examination of tropical and extratropical gust factors and the associated wind speed histograms. *Journal of Applied Meteorology* 44:270–280.
26. Schroeder J, Smith D, Peterson R (1998) Variation of turbulence intensities and integral scales during the passage of a hurricane. *J Wind Eng Ind Aerod* 77:65–72.
27. Wang B, Hu F, Cheng X (2011) Wind gust and turbulence statistics of typhoons in South China. *Acta Meteorolica Sinica* 25:113–127.
28. Sørensen J, Tarp-Johansen N (2005) Reliability-based optimization and optimal reliability level of offshore wind turbines. *Int J Offshore Polar* 15:141–146.

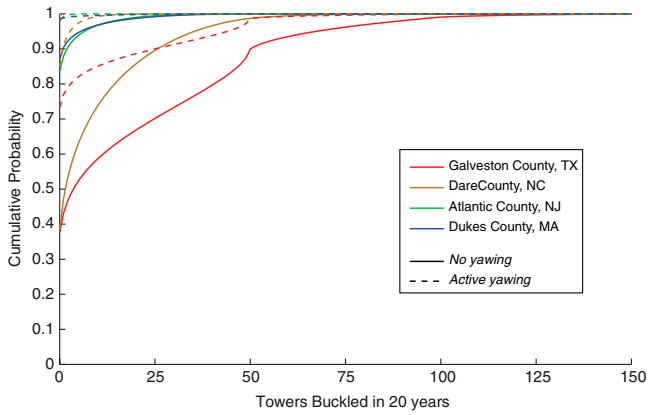

Fig. S1. Cumulative distribution of the number of towers in a 50-turbine wind farm buckled in 20 y if buckled towers are replaced after each storm if they buckle. Dashed lines plot the distribution for the case that turbines can yaw to track the wind direction, and solid lines plot the distribution for the case that turbines cannot yaw.

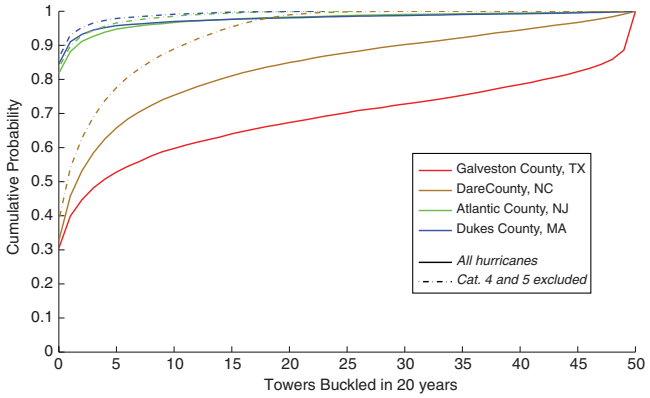

Fig. S2. CDF of the number of turbine towers buckled in 20 y without replacement; turbines cannot yaw to track the wind. Solid lines plot the distribution including all hurricanes, and dotted lines plot the distribution with Category 4 and 5 hurricanes excluded.

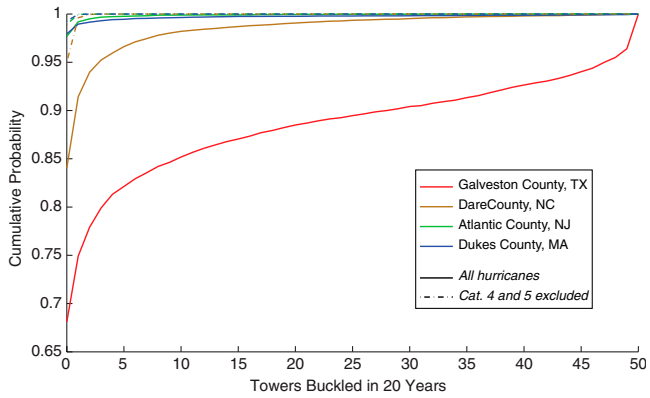

Fig. S3. CDF of the number of turbine towers buckled in 20 y without replacement; turbines can actively yaw to track the wind. Solid lines plot the distribution including all hurricanes, and dotted lines plot the distribution with Category 4 and 5 hurricanes excluded.

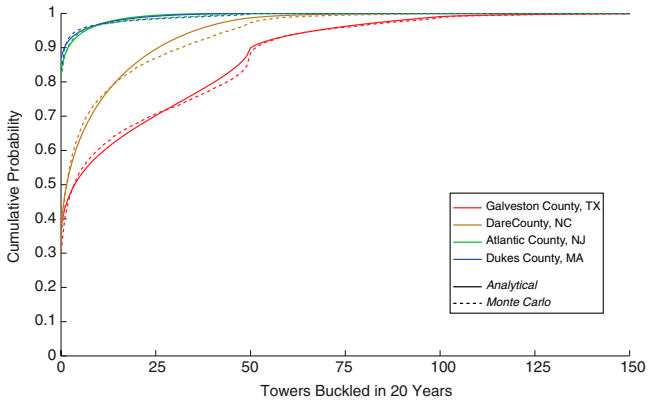

Fig. S4. A comparison of the cumulative probability distributions of number of turbine towers buckled in 20 y for the case where turbine towers are replaced after each storm if they buckle. Results calculated with Monte Carlo simulation are plotted as dashed lines and results calculated with a compound Poisson distribution are plotted as solid lines.

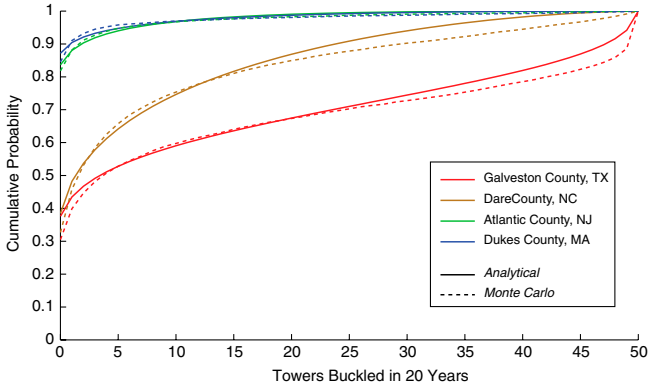

Fig. S5. A comparison of the cumulative probability distributions of number of turbine towers buckled in 20 y for the case where towers are not replaced if they buckle. Results calculated with Monte Carlo simulation are plotted as dashed lines and results calculated with a phase-type distribution are plotted as solid lines.

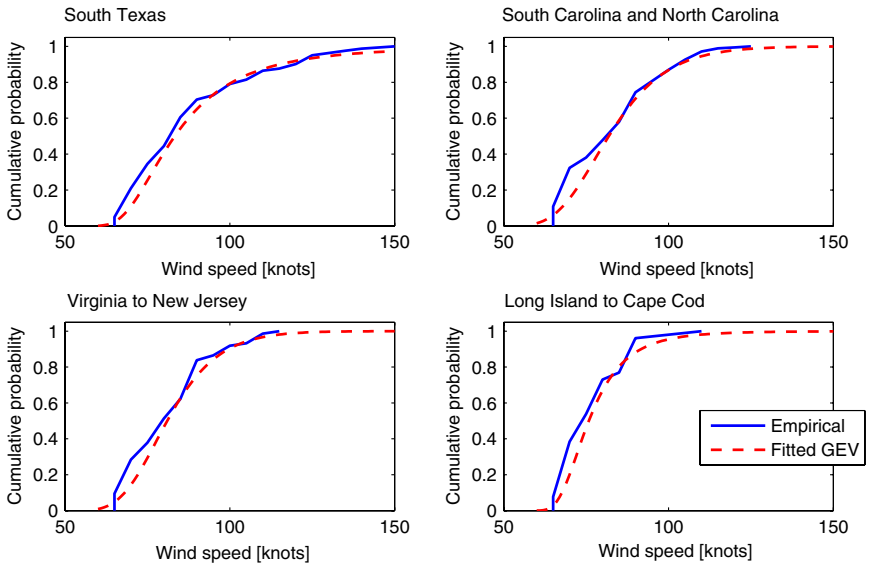

Fig. S6. Comparison of empirical CDFs for maximum hurricane wind speed in the regions we examine and the GEV distributions fitted to those data.

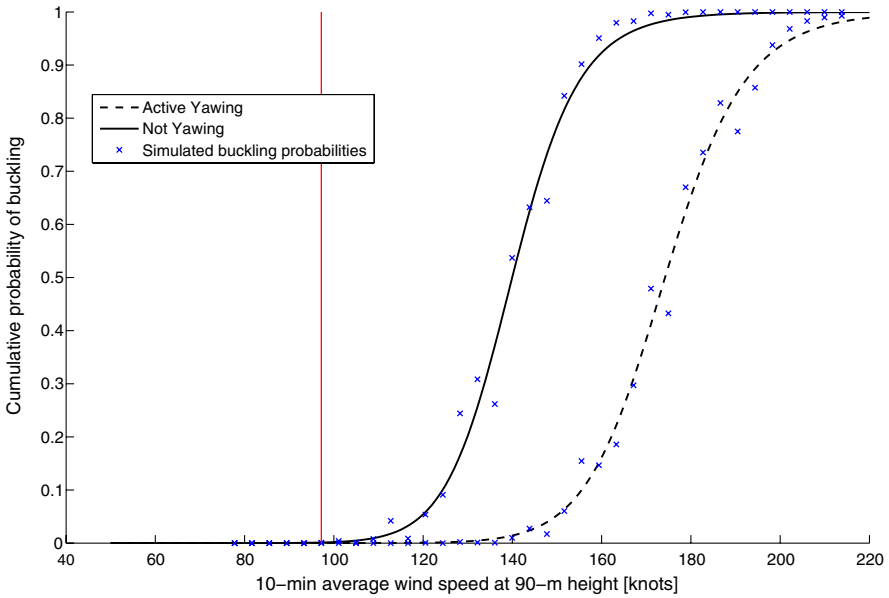

Fig. S7. Log-logistic functions fitted to probability of tower buckling as a function of wind speed. The vertical red line at 95 knots plots the 10-min sustained wind speed with a 50-y return period used to design Class I wind turbines in the IEC 61400-3 standard.

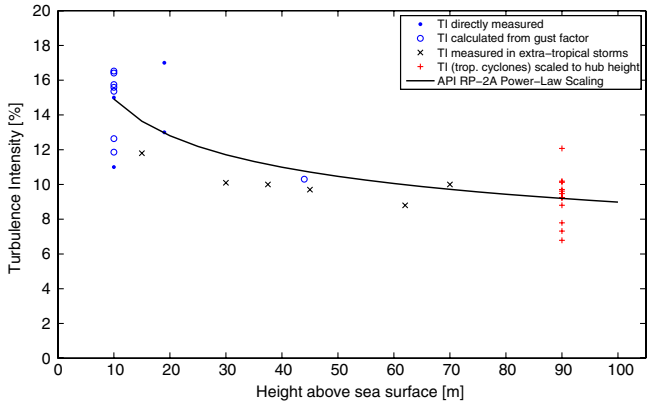

Fig. S8. TI in overwater tropical cyclones vs. height. TI values from tropical cyclones are scaled to 90-m height using a power-law relationship adapted from equation 2.3.2-3 in the API RP-2A-WSD standard. TI values measured in extratropical storms in the North Sea are also shown for comparison.

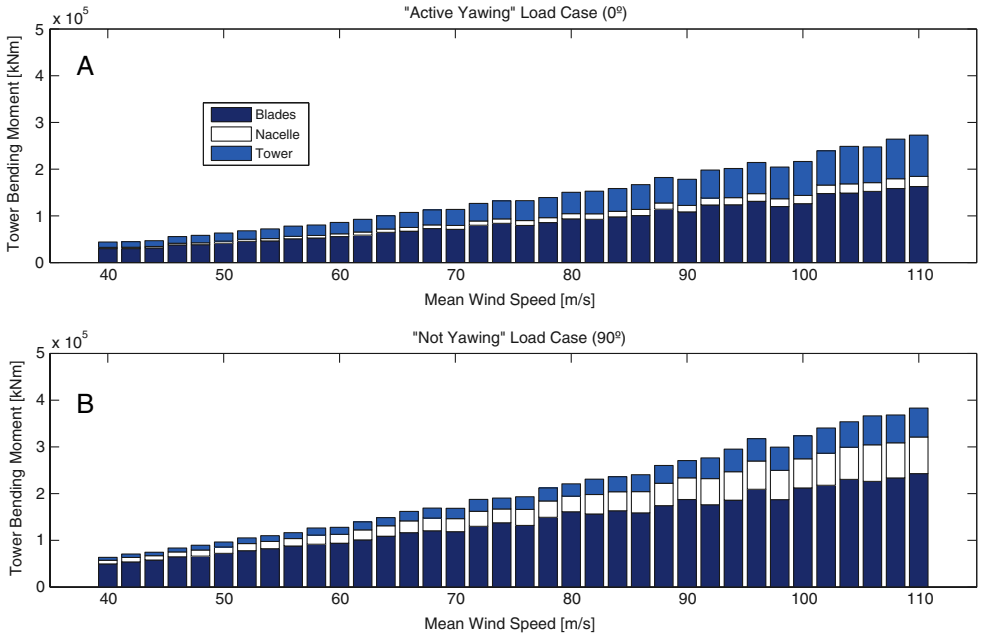

Fig. S9. Magnitude of bending moment on the tower base vs. 10-min mean wind speed. The "Blades" component of the moment is simulated using the NREL FAST software. The "Nacelle" component is calculated using [**S8**] the "Tower" component is calculated using [**S10**].

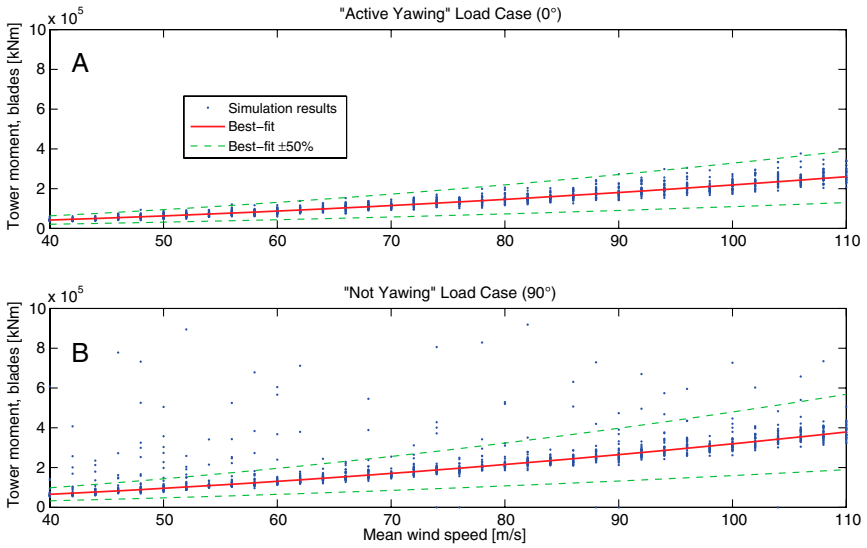

Fig. S10. The method for excluding anomalous simulation results for maximum tower bending moment. The red line is a robust linear best-fit to the data and the green dashed lines are 0.5 and 1.5 times the best-fit line. Data outside the green dashed lines are excluded.

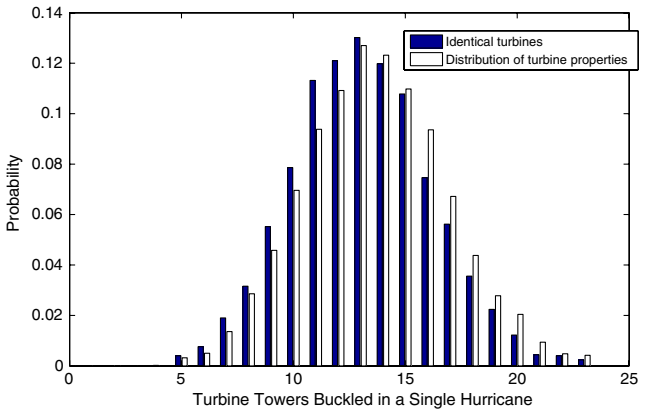

Fig. S11. Distribution of number of turbine towers buckled in a single hurricane a mean wind speed of 70 m/s (136 knots). Blue bars plot results for the case used in our paper, where buckling probabilities are identical for all turbines. White bars plot results for the case where the resistance to buckling of each tower is drawn randomly from the distribution given in [**S11**].

Table S1. 10-min turbulence intensities measured for hurricanes over water

TI	Measurement height	Source
15%	10 m	(25) Table 6
11%	10 m	(16) Table 2
13%	19 m	(26) Fig. 1
17%	19 m	(26) Fig. 1

Table S2. 10-min turbulence intensities calculated from GFs of hurricanes over water

GF	Calculated TI (10-min)	Measurement height	Source	Notes
1.4	16%	10 m	(27) Table 2	
1.38	16%	10 m	(27) Table 2	
1.45	15%	10 m	(17) Table 4	60-min averaging period
1.32	10%	44 m	(17) Table 4	60-min averaging period
1.46	16%	10 m	(17) Table 4	60-min averaging period
1.36	12%	10 m	(17) Table 4	60-min averaging period
1.38	13%	10 m	(17) Table 4	60-min averaging period
1.48	17%	10 m	(17) Table 4	60-min averaging period

Turbulence intensities are related to GF by the relation $\mathrm{TI} = (\mathrm{GF} - 1)/\alpha$, where $\alpha = 2.44$, an average of measured values from figure 7 in the paper by Yu, et al. (16). GF calculated from 60-min periods are converted to 10-min periods by dividing by 1.055, as recommended by Vickery (17).

Table S3. Parameters of wind load on nacelle

Parameter	Value	Description
ρ_a	1.21 kg/m^3	density of dry air at 20 °C
h_{max}	90 m	tower height
C_{front}	0.7	shape coefficient, nacelle front
C_{side}	1.2	shape coefficient, nacelle side
S_{front}	36 m^2	nacelle surface area, front
S_{side}	108 m^2	nacelle surface area, side

Table S4. Parameters of resistance to buckling at the base of a NREL 5-MW turbine tower. LN = log-normal **distribution, COV** = coefficient of variance

Variable	Description	Distribution type	Expected value	COV
D_{base}	tower diameter (base)	-	6 m	-
D_{top}	tower diameter (top)	-	3.87 m	-
t	tower thickness (base)	-	0.027 m	-
E	Young's modulus	-	210 GPa	-
F_y	yield stress	LN	1	0.05
$X_{y,ss}$	model uncertainties due to scale effects: yield stress	LN	1	0.05
$X_{E,ss}$	model uncertainties due to scale effects: Young's modulus	LN	1	0.02
X_{cr}	critical load capacity	LN	1	0.10

Adapted from ref. 28.